

# Journal of Materials Chemistry C

Accepted Manuscript



This is an *Accepted Manuscript*, which has been through the Royal Society of Chemistry peer review process and has been accepted for publication.

*Accepted Manuscripts* are published online shortly after acceptance, before technical editing, formatting and proof reading. Using this free service, authors can make their results available to the community, in citable form, before we publish the edited article. We will replace this *Accepted Manuscript* with the edited and formatted *Advance Article* as soon as it is available.

You can find more information about *Accepted Manuscripts* in the [Information for Authors](#).

Please note that technical editing may introduce minor changes to the text and/or graphics, which may alter content. The journal's standard [Terms & Conditions](#) and the [Ethical guidelines](#) still apply. In no event shall the Royal Society of Chemistry be held responsible for any errors or omissions in this *Accepted Manuscript* or any consequences arising from the use of any information it contains.

# An Electroless-Plating-Like Solution Deposition Approach for Large-Area Flexible Thin Film of Transition Metal Oxide Nanocrystals

Liangzhuan Wu, Yuan Yu,\* Xianying Han, Yuan Zhang, Yang Zhang, Yuzhen Li, Jinfang Zhi\*

Key Laboratory of Photochemical Conversion and Optoelectronic Materials, Technical Institute of Physics and Chemistry, Chinese Academy of Sciences, Beijing, 100190, P. R. China,

## Abstract

We developed a novel Electroless-Plating-Like Solution Deposition (EPLSD) approach for realization of large-area flexible thin films of transition metal oxides (TMOs) with  $d^0$  configuration. This EPLSD approach was triggered at  $80^\circ\text{C}$  through the redox reaction between Peroxo-Meal-Complex (PMC, including Peroxo-Titanium-Complex (PTC), Peroxo-Vanadium-Complex (PVC), and Peroxo-Molybdenum-Complex (PMoC)) and organic conductive electroactive polymer monomers (EDOT, Pyrrole, and Aniline). In the typical EPLSD process, a layer of organic conductive electroactive polymer monomers were absorbed onto the surface of the flexible polymer substrate by dip coating, and these pretreated flexible substrates were then immersed into an aqueous PMC solution for the EPLSD process. After the EPLSD process at  $80^\circ\text{C}$  for 30 min, large area (40cmx300cm) flexible thin films of metal oxide nanocrystals, including  $\text{TiO}_x$ ,  $\text{VO}_x$ , and  $\text{MoO}_x$ , nanocrystals films can be achieved. This low-temperature EPLSD process is advantageous for the flexible substrates and may easily realize TMOs film on the flexible substrates with different geometric shapes.

## I. Introduction

During the last few years, transition metal oxides (TMOs) such as titanium dioxide ( $\text{TiO}_2$ ), molybdenum tri-oxide ( $\text{MoO}_3$ ), vanadium pent-oxide ( $\text{V}_2\text{O}_5$ ) and tungsten tri-oxide ( $\text{WO}_3$ ) have been extensively studied because of their exceptional electronic properties<sup>1,2</sup> and their good transparency for electrodes<sup>3</sup>

or for charge generation/ recombination materials.<sup>4,5</sup> Meanwhile the flexible TMOs film is of great importance for the photocatalytic film,<sup>6</sup> electrochromic,<sup>7</sup> and flexible solar cell,<sup>8</sup> organic photovoltaic (OPV)<sup>9</sup> as well as in organic light emitting diodes (OLED) devices.<sup>10</sup> At present, TMOs films are usually deposited by using equipment-intensive techniques such as molecular beam epitaxy, electron beam evaporation, thermal evaporation, sputtering, pulsed laser deposition, etc.<sup>11,12</sup> The metal oxide films obtained from these approaches possess several advantages, including well controlled film thickness, high purity, and desired physical properties. However, atmospheric-pressure solution processing is still an attractive alternative to conventional vacuum-based deposition methods due to its ease of fabrication, scalability, and potential to lower device manufacturing cost.<sup>13</sup>

For large-scale and high-throughput production of flexible TMO films, solution processed approach is desired. More recently, Zilberberg et al. reviewed the synthesis and applications in organic electronic device of solution processed metal-oxides.<sup>14</sup> The ‘sol-gel’ processed inorganic metal oxide semiconductors have been intensively investigated for realizing large area flexible TMO film.<sup>15-20</sup> Crystalline metal oxides formed by the sol-gel route typically requires an annealing step at relatively high temperature, which is not compatible with conventional polymer substrates. For example, Hsu *et al.* reported crystalline MoO<sub>x</sub> thin film after 350 °C annealing post-treatment.<sup>21</sup> Ozer et al. sol-gel deposited amorphous VO<sub>x</sub> coatings by controlled hydrolytic condensation of vanadium(V) oxitriisopropoxide/isopropanol solution with addition of acetic acid acting as a catalyst and exchange ligand.<sup>22-24</sup> For the best homogeneity of the films, 250-300 °C firing was applied. To obtain flexible metal oxide films, some intricately modified sol-gel process were carried out to lower the annealing temperature. Marks *et al.*<sup>25</sup> reported a new strategy for fabricating solution-processed metal oxides film at the temperature as low as 200 °C using self-energy generating combustion chemistry, where the additional acetylaceton or urea was used as a “fuel” and metal nitrates as oxidizers. Kim *et al.* reported a

novel deep-ultraviolet-assisted sol-gel method for forming metal oxides flexible film at an unintentional annealing temperature up to  $\sim 150^\circ\text{C}$ , resulting from the radiant heat of the lamp.<sup>26</sup> It was particularly emphasized that TMO flexible films obtained through deep-ultraviolet-assisted sol-gel method are amorphous structure. The two modified sol-gel processes mentioned above required an additional post treatment. The former needs additional organic fuel and inorganic metal nitrates oxidizer to support the combustion chemistry process, and the later needs deep-ultraviolet annealing process and the as-prepared metal oxides are amorphous structure, and which complicate the application in a low-cost production scenario. Therefore, full realization of large-area, solution-processed crystalline metal oxide flexible films at the temperature lower than  $100^\circ\text{C}$  has remained challenging.

Electroless plating, also known as chemical or auto-catalytic plating, is a non-galvanic plating method that involves the simultaneous redox reactions between metal ions in an aqueous solution at room temperature for the realization of functional metal films. Could we realize the TMOs films on flexible polymer substrates through analogous approach? In this report, we reported a novel electroless-plating-like solution deposition (EPLSD) approach for preparing large-area flexible thin films of TMOs with  $d^0$  configuration. This EPLSD approach involves a key redox reaction between  $d^0$  configured PMC and the organic conduct electro-active polymer monomer (EDOT, Pyrrole, and Aniline), which was triggered at a low temperature of  $80^\circ\text{C}$ . By applying an EPLSD procedure, a PMC precursor (PTC, PVC or PMoC) can transform to corresponding TMOs crystals, and a flexible thin film of crystalline metal oxides, including  $\text{TiO}_x$ ,  $\text{VO}_x$ , and  $\text{MoO}_x$  can be obtained.

## II. Experimental Section

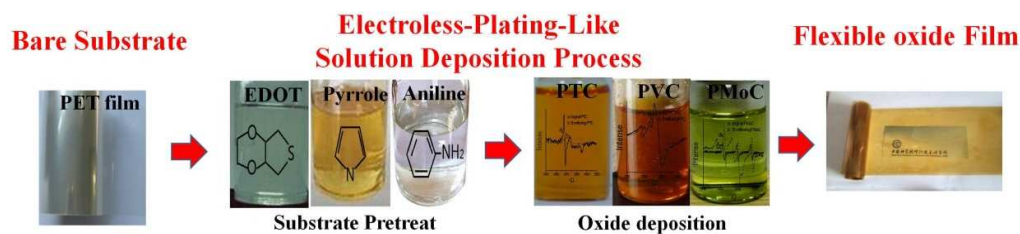


**Fig.1** Scheme of electroless-plating-like solution deposition (EPLSD) process for realization of large area crystalline transition metal oxides with  $d^0$  configuration flexible film.

All chemical reagents used in this experiment were analytical grade and purchased from Beijing chem. Co. Ltd. In a typical EPLSD process, as shown in Fig.1, the aniline, acted as polymer monomer, can be first absorbed onto the surface of flexible polymer substrates (PET film) by dip coating process due to their similar molecular polarity. The as-pretreated PET substrates were then immersed into the 80°C PMC aqueous (including PTC, PVC and PMoC) solution for 30 min to fulfill the EPLSD process. As a result, large area (40cm x 300cm in this report) TMOs nanocrystals films on PET substrates were implemented. In particular, this EPLSD approach may realize TMOs film on the flexible substrates with different geometric shapes, even with irregular shapes (tubular structure in this report). Powder X-ray diffraction (XRD) experiments were performed with a Rigaku D/max 2400 diffractometer using monochromatic  $\text{Cu K}\alpha$  radiation ( $\lambda=1.54 \text{ \AA}$ ), 40 kV and 120 mA, and scanning between  $5^\circ$  and  $50^\circ(2\theta)$ . Transmission electron microscopy (TEM) studies were performed using a Philips CM200/FEG field-emission-gun transmission electron microscope, operating at 200 kV.

### III. Results and Discussion

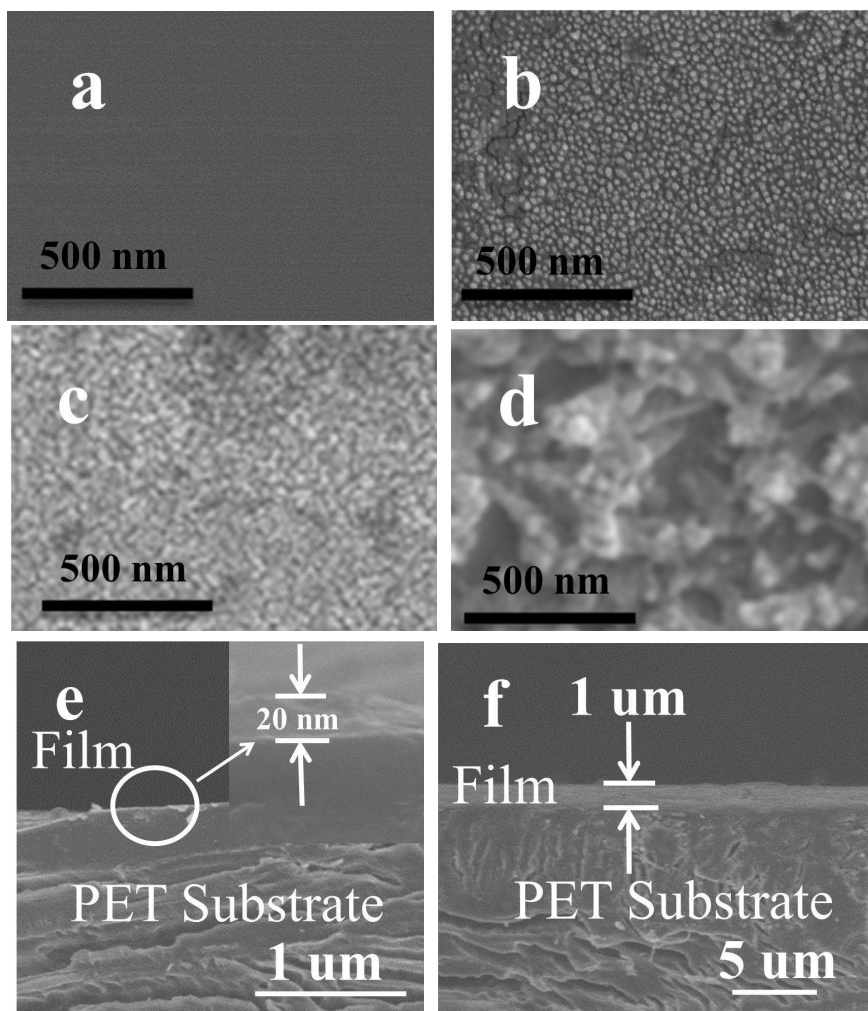


**Fig.2.** SEM images of the flexible film samples of (a) Natural PET film, (b), (c), and (d) Flexible PET films coated with  $\text{TiO}_x$ ,  $\text{VO}_x$ , and  $\text{MoO}_x$ , respectively; (e) and (f) The cross-section images of flexible  $\text{MoO}_x$  films obtained from EPLSD processes for 30 min and 10 h, respectively.

Fig.2 shows the SEM images of the obtained flexible PET film samples. These metal oxide films were prepared via the EPLSD processes that were triggered by the reactions between the corresponding PMC solution and the aniline molecules. As shown in Fig 2(a), the natural PET flexible film has a blank and smooth surface. Fig.2(b), (c) and (d) are the SEM images of the flexible PET films coated with  $\text{TiO}_x$ ,  $\text{VO}_x$ , and  $\text{MoO}_x$ , respectively. Compared to the natural PET film, the surfaces of PET films were completely covered with uniform nanocrystals. Although the atom ratios of metal/O were not consistent

with the chemical formula of  $\text{TiO}_2$ ,  $\text{V}_2\text{O}_5$ , and  $\text{MoO}_3$  due to the existence of the O atom in the substrate, the EDS (see supporting information) spectra analysis indicated that that these nanoparticles forming on the surface of the PET films were metals oxides of Ti, V and Mo, respectively. Fig.2(e) is the cross-section images of flexible  $\text{MoO}_x$  films obtained from EPLSD process for 30 min, showing the thickness of the flexible  $\text{MoO}_x$  film is about 20 nm (see the magnified part). When the EPLSD process prolongs to 10 h, the thickness of the flexible  $\text{MoO}_x$  film extended to 1  $\mu\text{m}$  (Fig.2(f)), suggesting that the thickness of the EPLSD processed flexible metal oxide films is controllable by adjusting the reaction time.

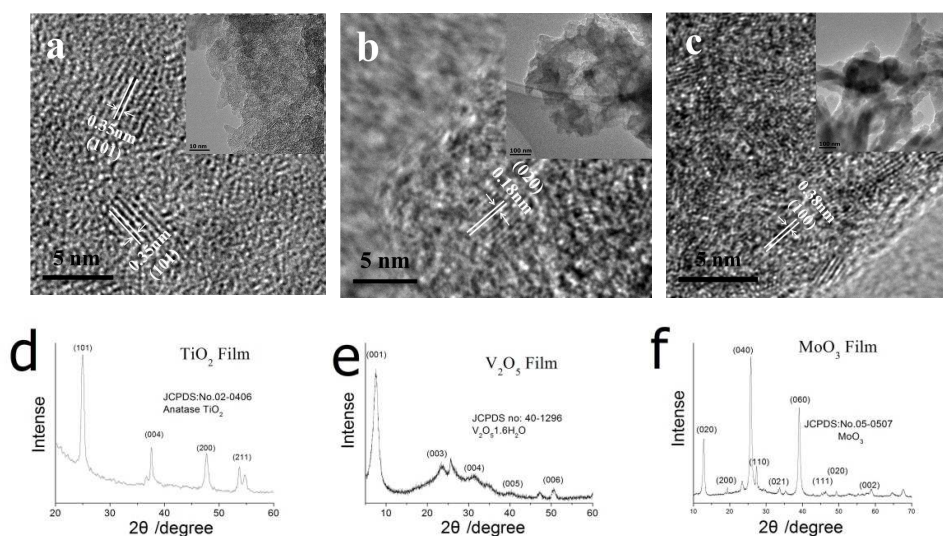


**Fig.3** Morphology and structure analysis of the samples that were scraped off from the PET films with a knife. TEM images of the as scraped off samples from the Flexible PET film coated with (a)  $\text{TiO}_x$ , (b)  $\text{VO}_x$ , and (c)  $\text{MoO}_x$ , and XRD pattern taken from the as scraped off samples of (d)  $\text{TiO}_x$  film, (e)  $\text{VO}_x$  film, and (f)  $\text{MoO}_x$  film, respectively.

Fig. 3(a), (b), and (c) are the corresponding HRTEM images taken from the samples that were scraped off the EPLSD processed PET films surface with a knife. The inset parts are corresponding low magnification images. All the three images showed that some crystalline nanoparticles with the size of

about 4-6 nm in diameters are surrounded by amorphous materials. The lattice planes shown in the HRTEM image corresponding to distances 0.35 nm agree well with distances of (101) lattice planes of anatase  $\text{TiO}_2$  (Fig. 3a) (JCPDS no: 02-0406), 0.18 nm corresponds to the (020) plane spacing of ortho-rhombic phase  $\text{V}_2\text{O}_5 \cdot 1.6\text{H}_2\text{O}$  (Fig. 3b) (JCPDS no: 40-1296), and 0.38 nm corresponds to (100) plane spacing of  $\text{MoO}_3$  (Fig. 3c) (JCPDS no: 05-0507) respectively. HRTEM images revealed that these crystalline nanoparticles were  $\text{TiO}_2$ ,  $\text{V}_2\text{O}_5$ , and  $\text{MoO}_3$  nanocrystals. Fig. 3(d), (e), and (f) shows the corresponding XRD patterns of the scraped off samples. As shown in Fig. 3d, all the diffraction peaks of the nanoparticle samples scraped from the PTC EPLSD processed PET film are the pure anatase crystalline phase of titania (JCPDS no: 02-0406). Similar to the PTC based EPLSD processed sample, as was shown in Fig. 3e and 3f, all the Bragg peaks of nanoparticles samples originated from the PVC (Fig. 3e) and PMoC (Fig. 3f) processed PET substrates are consistent with those of the ortho-rhombic phase  $\text{V}_2\text{O}_5 \cdot 1.6\text{H}_2\text{O}$  (Fig. 3e) (JCPDS no: 40-1296), and  $\text{MoO}_3$  (Fig. 3f) (JCPDS no: 05-0507) respectively. It verifies that the nanocrystals of the metal oxides can be deposited onto the surface of PET films through the EPLSD process. By changing conductive electroactive polymer monomer from aniline to EDOT and Pyrrole (Py) in the EPLSD process (PTC), as shown in supporting information S1, the crystalline anatase  $\text{TiO}_2$  nanoparticles of about 6 nm in diameter were deposited onto the surface, verifying that EDOT and Pyrrole, like the Aniline, can also be used to deposit metal oxide onto the surface of PET films through the EPLSD process. Although both HRTEM and XRD data verified that the main structures of the TMOs agreed with the stoichiometric  $\text{TiO}_2$ ,  $\text{V}_2\text{O}_5$ , and  $\text{MoO}_3$ , we cannot exclude the possibility of the existence of non-stoichiometric TMOs due to the limitation of the detection range.

Furthermore, FTIR results (see supporting information S2) of the EPLSD-processed  $\text{TiO}_x$  film samples obtained from the reaction between PTC and aniline showed that the polyaniline was generated during the EPLSD process. Therefore, the amorphous structure shown in Fig. 3 might be polyaniline. In addition,



XPS was used to clarify the relationship between the polyaniline and  $\text{TiO}_x$ . As was shown in supporting information S3, XPS peaks shifting suggested that a Ti-O-N-C and Ti-O-C bonding may be generated between PANi and  $\text{TiO}_x$  nanocrystals, which could explain the strong adhesion between the metal oxides and the PET substrates.

Up to now, we can preliminarily interpret the attachment of metal oxide nanocrystals onto the PET film surface through the EPLSD process. By dipping the PET film into the solution of conductive electroactive polymer monomer, a layer of organic monomer molecules can be absorbed onto the PET surface due to the similar polarity (like dissolves like). During the EPLSD process, the small organic molecule monomer layer on the surface of PET was changed to corresponding polymer via chemical oxidative polymerization process, since PMC has good water solubility and strong oxidizability. The PMC were reduced to the corresponding metal oxide. The *in-situ* produced polymer could be regard as a self-binder reagent, and this process makes the metal oxides attached on the surface of PET firmly.

However, there are still two questions related to the EPLSD process to be answered, that are, why only the  $d^0$  configured TMO can be obtained through this EPLSD process, and why the crystalline TMO can be deposited at a lower temperature ( $80^\circ\text{C}$ ). For the first question, it is well known that the polymer product can be easily obtained from the conductive electro-active monomer through the radical polymerization by using peroxide (such as the ammonium persulfate, benzoyl peroxide) as radical initiator. Interestingly, the  $\text{MO}\cdot$  radicals signals of  $\text{TiO}\cdot$ ,  $\text{VO}\cdot$  and  $\text{MoO}\cdot$  can be detected in the PTC, PVC and PMoC precursors using Electron Spin Resonance (ESR) (see supporting information S4) during the reaction process. It is thus reasonable to conclude that the redox reaction between the PMC and conductive electro-active monomer (aniline, pyrrole and EDOT) used in present EPLSD process should follow on a radical polymerization process. Through this radical polymerization reaction, PMC was reduced to metal oxides, and the small organic molecular monomer was polymerized into polymer. The

as-produced polymer acts as a self-binder to make the metal oxide attach on the surface of PET film adhesively.

On the other hand, only for the early transition metal series in their highest oxidation states (with  $d^0$  configuration (Ti(IV), V(V), Mo(VI)), the  $MO\bullet$  radicals, which was necessary for the radical polymerization process, can be generated by the homolytic cleavage of peroxy group. While for the early transition metal series with  $d^x$  configuration (possessed valence electrons in d electron orbit), according to the Fenton-Haber-Weiss mechanism, an easily and rapidly electron transfer between the peroxy group complex and the central metal ions will occur, leading to a rapid heterolytic cleavage reaction of peroxy group. Therefore, the unstable  $d^x$  configured PMC cannot be used for the EPLSD process due to the failure in generating  $MO\bullet$  radicals.

In addition, concerning on the low reaction temperature of the EPLSD process, it is interesting to notice that the  $80\text{ }^\circ\text{C}$  operating temperature is even lower than the refluxing temperature ( $100\text{ }^\circ\text{C}$ ), It is thus important to understand the reaction mechanism involved in EPLSD process.

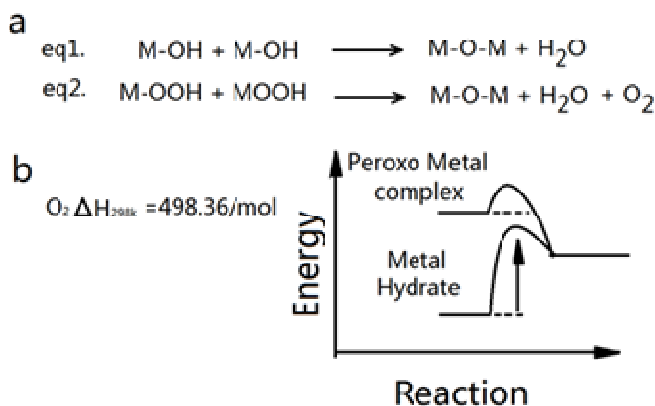


**Fig.4** The mechanism of metal oxides preparing from metal hydrate and PMC solution, respectively. (a) The chemical equations of the two metal oxide generated reactions. (b) Energetics of PMC based homolytic cleavage reaction versus the conventional condensation process of metal hydrate.

As shown in Fig.4a, As described above, we think that the metal oxides deposited onto the PET films

are the results of a radical redox reaction process which relies upon the condensation of  $\text{MO}\cdot$  radicals. Through this radical polymerization reaction, PMC was reduced to metal oxides, and the small organic molecular monomer was oxidized and further polymerized into polymer. It is different from those obtained from the condensation process of the conventional metal hydrate precursor, which usually need high annealing temperature to trigger the reaction and support the crystallization process (Fig. 4a). As showed in Fig4b, in the condensation process of  $\text{MO}\cdot$  radicals, an extra exothermic of  $\Delta H_{298\text{k}}=498.63\text{KJ}$  can be obtained by the decomposition of peroxy group, and this self-generated energy can support the the formation of metal-O-metal crystalline lattice. That is, reaction–self provides a localized energy supply, eliminating the need of high, externally applied temperatures. Therefore, the low temperature of  $80^\circ\text{C}$ , is only the needed temperature for triggering the reaction between the PMC and the polymer monomer. While the metal oxides formation via the condensation process of the conventional metal hydrate precursor is endothermic, requiring significant external energy input to form crystalline metal-O-metal lattice. The organic monomer plays an important role on the EPLSD process. In order to initiate a homolytic cleavage of peroxy group in PMC to generate  $\text{MO}\cdot$  radicals, the redox cleavage process by the monomer is necessary. In a word, the monomer indeed acts as a kind of reducing agent in the reaction between PMC and monomer. During the EPLSD process, the PMC was reduced to TMOs nanocrystals, and the monomer was oxidized and further polymerized into polymer.

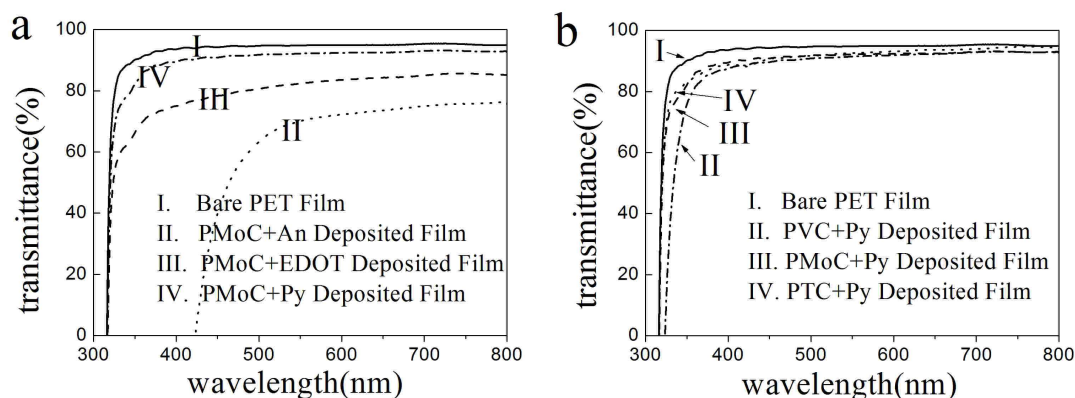


**Fig.5** Transmittance of the EPLSD-processed flexible metal oxide films (irradiation wavelength: 300~800 nm) obtained from (a): the reaction between PMoC solution and different monomers, including Ani, EDOT, and Py monomers. (b): the reaction between different PMC solutions (including PTC, PVC and PMoC) and Py monomer.

The transmittances of the EPLSD-processed flexible metal oxide films obtained under different reactions were monitored by UV-Vs spectrometer under the irradiation wavelength of 300nm~800nm. Fig.5(a) shows the transmittance of the EPLSD-processed flexible metal oxide films obtained from the reactions between PMoC solution and different monomers, including Ani, EDOT, and Py monomers, revealing that the Py-induced MoO<sub>x</sub> flexible film possess the best translucent, and it displays the transmittance of about 90 % at 380-800 nm light irradiation wavelengths. As shown in Fig.5(b), Py-induced TiO<sub>x</sub> and VO<sub>x</sub> flexible films has the same results, and both their transmittance are higher than 90% at 380-800 nm light irradiation wavelengths. Compared to Py-induced MoO<sub>x</sub> flexible, the transmittances of Ani- and EDOT-induced MoO<sub>x</sub> flexible films have an obvious decrease. The EDOT-induced MoO<sub>x</sub> flexible film displays the transmittance of about 80 % at 480-800 nm light irradiation wavelengths, and Ani- induced MoO<sub>x</sub> flexible film displays the transmittance of about 70 % at 560-800 nm light irradiation wavelengths. The transmittance experiments show that the Py-induced metal oxide flexible film possesses the best translucent.

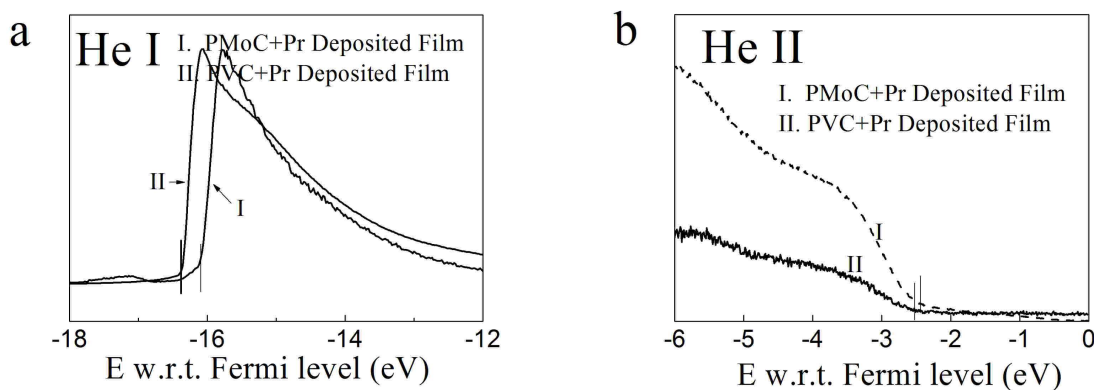


**Fig. 6** UPS spectra of the EPLSD-processed MoO<sub>x</sub> and VO<sub>x</sub> films: (a) He I spectra and (b) He II spectra.

Position of gap states marked with arrows.

Fig. 6(a) shows the UPS spectra (He I) of the EPLSD-processed VO<sub>x</sub> and MoO<sub>x</sub> flexible films. The photoemission onsets of the VO<sub>x</sub> film and MoO<sub>x</sub> in He I spectra are respectively at 16.4 eV and 15.8 eV, giving the VO<sub>x</sub> film work-function (WF) of 4.8 eV, and MoO<sub>x</sub> film WF of 5.4 eV. Shown in Fig. 8(b) are the UPS (He II) spectra of the VO<sub>x</sub> and MoO<sub>x</sub> flexible film, displaying the bandgap of VO<sub>x</sub> and MoO<sub>x</sub> flexible film are of about 2.5 eV, and 2.3eV, respectively.

To test the properties of the flexible film of metal oxides, the photocatalytic activities of the as prepared Ani-induced TiO<sub>x</sub> film were evaluated by methylene blue degradation in an aqueous solution (see supporting information S5). In a typical experiment, the films slides (25 mm × 40 mm) were then dipped in 5 × 10<sup>-5</sup> M methylene blue for 8 h to obtain the equilibrium adsorption of methylene blue, then put into a watch glass containing 20 mL of 1 × 10<sup>-5</sup> M methylene blue solution and exposed to the 365 nm UV light for 120 min. The result of MB degradation tests revealed that the TiO<sub>x</sub> coated PET film demonstrated an obvious photocatalytic activity (8% MB concentration decrease) compared with a photocatalytic inactivity bare PET film.

#### IV. Conclusions

A novel EPLSD approach for realization of large-area flexible thin films of metal oxides with d<sup>0</sup> configuration has been developed. This EPLSD approach involves a key reaction between d<sup>0</sup> configured PMC and conductive electroactive polymer monomer molecules. The redox radical polymerization process was triggered at the low temperature as low as 80°C, and the self-generated energy is responsible for the formation of the crystalline metal-O-metal lattice. This EPLSD process can realize large-area and low-cost the production of TiO<sub>x</sub>, VO<sub>x</sub>, and MoO<sub>x</sub> flexible films, representing a promising step toward flexible electronics.

#### Corresponding Author

Address correspondence to either author. Phone: 86-010-83543537. Fax: 86-010-62554670. Email:

yyu@mail.ipc.ac.cn (Y. Yu); Zhi-mail@mail.ipc.ac.cn (J. Zhi).

### Acknowledgement

The authors appreciate the supports of the International Science & Technology Cooperation Program of China (no. 2013DFG50150), the Natural Foundation of Sciences of the People's Republic of China (Grant no. 21175144, and 20903111 ) and the Key Project of Beijing Natural Science Foundation (Grant No. 2120002).

### References

1. M. T. Greiner, M. G. Helander, W.-M. Tang, Z.-B. Wang, J. Qiu, Z.-H. Lu, *Nat. Mater.*, 2012, **11**, 76-81.
2. D. Cahen, A. Kahn, *Adv. Mater.*, 2003, **15**, 271–277 .
3. T. Wehlius, T. Korner, S. Nowy, J. Frischeisen, H. Karl, B. Stritzker, W. Brütting, *Phys. Status Solidi A*, 2011, **208**, 264-275.
4. T. W. Lee, T. Noh, B. K. Choi, M. S. Kim, D. W. Shin, J. Kido, *Appl. Phys. Lett.*, 2008, **92**, 043301.
5. C. H. Chou, W. L. Kwan, Z. Hong, L. M. Chen, Y. Yang , *Adv. Mater.* **23** , 1282–1286(2011)
6. Y. Li, Y. Yu, J. Zhi, *App. Surf. Sci.*, 2013, **273**, 173-178.
7. R. J. Colton, A. M. Guzman, J. W. Rabalais, *Acc. Chem. Res.*, 1978, **11**, 170–176.
8. G. orotcenkov, *Mater. Sci. Eng. B*, 2007, **139**, 1-23.
9. Y. Li, D.-K. Lee, J. Y. Kim, B. S. Kim, N.-G. Park, K. Kim, J.-H. Shin, I.-S. Choi and M. J. Ko, *Energy Environ. Sci.*, 2012, **5**, 8950-8957.
10. L. M. Chen, Z. R. Hong, G. Li , Y. Yang, *Adv. Mater.*, 2009, **21**, 1434–1449.
11. J. Meyer, S. Hamwi, T. Bülow, H. H. Johannes, T. Riedl, W. Kowalsky, *Appl. Phys. Lett.*, 2007, **91**, 113506.

12. S. M. Pawar, B. Pawar, J. H. Kim, S. Joo and C. Lokhande, *Curr. Appl. Phys.*, 2011, **11**, 117–161.
13. Robert M. Pasquarelli, D. S. Ginley, R. O'Hayre, *Chem. Soc. Rev.*, 2011, **40**, 5406-5441.
14. K. Zilberberg, J. Mery, and T. Riedl, *J. Mater. Chem. C*, 2013, **1**, 4796-4815.
15. K. X. Steirer, P. F. Ndione, N. E. Widjonarko, M. T. Lloyd, J. Meyer, E. L. Ratcliff, A. Kahn, N. R. Armstrong, C. J. Curtis, D. S. Ginley, J. J. Berry, D. C. Olson, *Adv. Energy Mater.*, 2011, **1**, 813–820.
16. E. L. Ratcliff, J. Meyer, K. X. Steirer, A. Garcia, J. J. Berry, D. S. Ginley, D. C. Olson, A. Kahn, N. R. Armstrong, *Chem. Mater.*, 2011, **23**, 4988-5000.
17. K. Zilberberg, S. Trost, H. Schmidt, T. Riedl, *Adv. Energy Mater.*, 2011, **1**, 377-381.
18. C.-P. Chen, Y.-D. Chen, S.-C. Chuang, *Adv. Mater.*, 2011, **23**, 3859–3863.
19. M. Campoy-Quiles, T. Ferenczi, T. Agostinelli, P. G. Etchegoin, Y. Kim, T. D. Anthopoulos, P. N. Stavrinou, D. D. C. Bradley, and J. Nelson, *Nat. Mater.*, 2008, **7**, 158-164.
20. K. Zilberberg, S. Trost, J. Meyer, A. Kahn, A. Behrendt, D. Lutzenkirchen-Hecht, R. Frahm, T. Riedl, *Adv. Funct. Mater.*, 2011, **21**, 4776-4783
21. C. S. Hsu, C. C. Chan, H. T. Huang, C. H. Peng, and W. C. Hsu, *Thin Solid Films*, 2008, **516**, 4839-4844..
22. N. Ozer and C. M. Lampert, *Thin Solid Films*, 1999, **349**, 205–211.
23. N. Ozer and C. M. Lampert, *Sol. Energy Mater. Sol. Cells*, 1998, **54**, 147–156.
24. N. Ozer, *Thin Solid Films*, 1997, **305**, 80–87.
25. M-G Kim, M. G. Kanatzidis, A. Facchetti, and T. J. Marks, *Nat. Mater.*, 2011, **10**, 382-388.
26. Y. H. Kim, J. S. Heo, T. H. Kim, S. Park, M. H. Yoon, J. Kim, M. S. Oh, G. Yi, Y. Noh and S. K. Park, *Nature*, 2012, **489**, 128-132..

